Original Article

DOI: 10.5582/ddt.2023.01047

Quercetin antagonized advanced glycated end products induced apoptosis and functional inhibition of fibroblasts from the prolapsed uterosacral ligament

Yizhen Sima[1,2,3,4,§], Junwei Li[1,§], Leimei Xu[1,§], Chengzhen Xiao[1], Lisha Li[2,3,4], Ling Wang[2,3,4,*], Yisong Chen[1,*]

[1] Department of Gynecology, Obstetrics and Gynecology Hospital of Fudan University, Shanghai, China;
[2] Laboratory for Reproductive Immunology, Obstetrics and Gynecology Hospital of Fudan University, Shanghai, China;
[3] The Academy of Integrative Medicine of Fudan University, Shanghai, China;
[4] Shanghai Key Laboratory of Female Reproductive Endocrine-related Diseases, Shanghai, China.

SUMMARY The altered behaviors and functions of pelvic floor fibroblasts are pathophysiological changes of pelvic organ prolapse (POP). Our previous study showed that advanced glycated end products (AGEs) accumulated in the pelvic tissues of POP and induced fibroblast apoptosis. The study was designed to investigate whether quercetin antagonize AGEs-induced apoptosis and functional inhibition of fibroblasts. The uptake of 5-ethynyl-2'-deoxyuridine (EdU) was evaluated for cell proliferation. Flow cytometric analysis was applied for cell apoptosis. Intracellular reactive oxygen species (ROS) content was determined by the fluorescence of dichlorofluorescein (DCF). The contractility of fibroblasts was measured by collagen gel contraction assay. The expressions of extracellular matrix (ECM) related genes and the expression of miR-4429 and caspase-3 were quantified by qPCR. The expressions of phosphatase and tensin homolog (PTEN), phosphoinositide 3-kinase (PI3K), serine-threonine kinase (Akt), and phosphorylated Akt (p-Akt) were analyzed by Western Blot. The down-regulation of miR-4429 was achieved by cell transfection. Quercetin antagonized AGEs-induced apoptosis, proliferation inhibition, and ROS increase in fibroblasts. Quercetin did not alleviate AGEs-induced contractile impairment of fibroblasts. Quercetin reduced the gene expressions of lysyl oxidase like protein 1 (LOXL1) and matrix metallopeptidase 1 (MMP1), and increased the gene expressions of lysyl oxidase (LOX) and fibrillin 2 (FBN2) in fibroblasts. Quercetin reversed AGEs-induced upregulation of PTEN and downregulation of PI3K, P-Akt, and miR-4429 in fibroblasts. The inhibitory effect of quercetin on AGEs-induced fibroblast apoptosis was inhibited by downregulating the expression of miR-4429. In conclusion, quercetin antagonized AGEs-induced apoptosis and functional inhibition of fibroblasts from the prolapsed uterosacral ligament. And inhibiting AGEs-induced down-regulation of miR-4429/PTEN/PI3K/Akt pathway was the mechanism underlying the antagonistic effect of quercetin on AGEs-induced apoptosis.

Keywords pelvic organ prolapse, quercetin, fibroblasts, advanced glycation end products

1. Introduction

Pelvic organ prolapse (POP), caused by damages or weakness of the pelvic supportive tissues, is a common degenerative disease in women. The incidence of symptomatic POP was 9.6% in Chinese women over the age of 20 (*1*). Given the high prevalence, the pathophysiology of POP has not been understood. The abnormal contents and structures of collagen and elastic fibers in pelvic floor connective tissues lead to the decrease of mechanical strength for pelvic organs. Pelvic supportive tissues include the levator ani muscle complex and connective-tissue attachments of the pelvic organs (*2*). Fibroblasts are responsible for the regulation of extracellular matrix (ECM) that determines the mechanical properties of pelvic connective tissues. The previous studies reported functional differences among cell proliferation, contractility, adhesion, oxidative stress, and ECM metabolism between fibroblasts from the prolapsed and normal tissues (*3-7*). Therefore, investigation on fibroblasts is important to reveal the reasons behind the impaired supportive structures in

POP.

Advanced glycation end products (AGEs) refer to a heterogeneous group of glycation adducts of proteins by glucose or other saccharides. AGEs could induce a series of cell inflammation and oxidative stress and have been extensively investigated in diabetes mellitus (*8,9*). In addition, AGEs affected the metabolism of collagens by accelerating collagen degeneration, resulting in tissue strength impaired, skin aging (*10*), and bone remodeling (*11*). In 1996, Jackson *et al.* first reported that the level of advanced glycation cross-links elevated in prolapsed vaginal-epithelial tissue (*12*). Our previous report indicated that AGEs content increased in the vaginal wall of the POP patients in contrasted with the non-POP patients (*13*). Then, several studies also found an elevated level of AGEs in the muscularis propria of vaginal wall among POP patients (*14,15*), but the mechanisms of AGEs participating in the development of POP were not studied. Similar to the pathogenesis in diabetes complications, we previously reported that AGEs reduced the type I collagen by increasing the expression of matrix metalloproteinase-1 (MMP-1) in human vaginal fibroblasts through the receptor for AGEs on cell membrane (*16*). In our recent study, we reported that AGEs induced the expression of phosphatase and tensin homolog (PTEN) *via* reducing the expression of miR-4429, thus suppressing the phosphoinositide 3-kinase (PI3K)/ serine-threonine kinase (Akt) pathway and induced fibroblast apoptosis (*17*).

Quercetin, as a widely studied natural flavonoid, was reported as an effective antioxidant, which improved renal function in diabetic nephropathy rats by inhibiting intracellular reactive oxygen species (ROS) (*18*) and ameliorated myocardial injury caused by oxidative stress (*19*). Oxidative stress is one of the factors leading to cellular senescence, and the role of quercetin in delaying cellular senescence has been studied. Quercetin delayed the senescence of skin fibroblasts by inhibiting the increase of intracellular H_2O_2 and iron death caused by UV irradiation (*20*). Quercetin selectively eliminated senescent cells, and its use in combination with dasatinib was known as Senolytics therapy (*21*). In the mouse model of idiopathic pulmonary fibrosis, quercetin induced the apoptosis of senescent fibroblasts to inhibit fibrosis (*22*). Aging is a risk factor for POP. In addition, senescence and oxidative stress of pelvic floor fibroblasts resulted in the apoptosis and dysregulation of ECM metabolism (*23,24*). Therefore, it is worth exploring whether quercetin achieve the therapeutic effect for POP by inhibiting the apoptosis of pelvic floor fibroblasts and maintaining ECM homeostasis. What's more, quercetin inhibits AGEs formation *via* chelating metal ions and trapping methylglyoxal (*25*). Previous studies reported that quercetin suppressed AGEs-induced cell apoptosis in human skin fibroblasts (*26*) and reversed dietary AGEs-induced cognitive dysfunction in aged mice (*27*).

The present study aimed to investigate whether quercetin antagonizes the apoptosis and functional inhibition of pelvic floor fibroblasts induced by AGEs, and further explore the mechanism of quercetin in antagonizing the apoptosis of fibroblasts. We isolated fibroblasts from the human uterosacral ligament in POP and non-POP patients and evaluated the influences of AGEs and quercetin on cell proliferation, apoptosis, ROS, contractility, and ECM production. We found that quercetin antagonized AGE-induced apoptosis and functional inhibition of fibroblasts. In addition, quercetin reduced the apoptosis of fibroblasts by inhibiting the AGEs-induced downregulation of the miR-4429/PTEN/PI3K/Akt pathway.

2. Materials and Methods

2.1. Ethics statement

Human protocols in current study were authorized by the local Ethics Committee of the Obstetrics and Gynecology Hospital of Fudan University (Shanghai, China). The number is 2021-234. The study included a total of 20 subjects who underwent a hysterectomy at the same hospital from January to October 2021. All subjects in the study had signed informed consent before the operations. The sample in the study was a piece of the uterosacral ligament with a size of 0.5 cm^2 which was cut from the removed uterus during operations.

2.2. Patients

There were 20 patients included in the POP and non-POP groups according to the inclusion and exclusion criteria, 10 patients in each group. Inclusion criteria of the POP group are including ≥ 45 years old, POP-Q (pelvic organ prolapsed quantification) ≥ stage III (*28,29*), and received hysterectomy. Inclusion criteria of the non-POP group are including ≥ 45 years old, without any pelvic organ prolapsed manifestation, received a hysterectomy at the same hospital due to other benign gynecological diseases (uterine fibroids, cervical precancerous lesions, endometrial lesions, postmenopausal ovarian benign tumors). Patients who had pelvic surgeries, pelvic inflammation, malignant diseases, severe systemic diseases, and with a history of hormone replacement therapy were ruled out. The clinical data files were collected from all the included patients and the information about age, body mass index, parity, and menopause rate were reported in our previous study (*17*).

2.3. Isolation and culture of the primary cells

Human uterosacral ligament fibroblasts were obtained from patients who underwent a hysterectomy. A piece of fresh tissue with a size of 0.5 cm^2 was collected after the removal of the uterus during the operation. The fresh

tissue specimens were washed with phosphate-buffered saline (PBS) containing 1% penicillin, streptomycin, and amphotericin B (Genom, Hangzhou, Zhejiang, China) and cut into 1 mm^3 pieces. Then the tissue pieces were put into the type I collagenase (Sigma-Aldrich, St. Louis, MO, USA) solution and shook up for 1 hour at 37°C. The digested mixture was centrifuged to collect the cell pellet. The cell pellet was resuspended in 1 mL of DMEM medium containing 20% fetal bovine serum (FBS) (Gibco, Grand Island, NY, USA) and 1% triple antibiotic (Genom) and transferred to six-well plates. The culture plates were placed in a cell incubator and the culture medium was changed when some adherent cells could be observed. From then on, the primary cells were cultured at 37°C in a 5% CO_2 atmosphere, and renewed the medium every 2-3 days. Identification of the primary fibroblasts was performed and the results were reported in the previous study (*17*). Fibroblasts were passaged at 80% confluency and the cells with passages 3-5 were used in the current study.

2.4. Cell apoptosis assay

Cell apoptosis assays were conducted by flow cytometric analysis using a fluorescein isothiocyanate (FITC) Annexin V/propidium iodide (PI) kit (BD Bioscience, San Jose, CA, USA) according to the manufacturer's instructions. Cultured fibroblasts were collected and washed by staining buffer (BD Bioscience) for 2 times. The cell suspension was centrifuged at 800× *g* for 5 min. Then FITC and PI were successively added into the 300 μL staining buffer to make cells stained by the fluorescence for 15 min and 10 min in dark at room temperature. All prepared cell samples were assayed by a flow cytometry (Becton Dickinson, Franklin Lakes, NJ, USA). The viable cells and apoptotic cells were distinguished by the detection of fluorescence signals. All data generated by flow cytometry were processed by the FlowJo version X.0.7. Number of positive cells was determined in comparison to the unstained cells as controls.

2.5. Cell proliferation assay

Proliferative capacity was assessed by the incorporation of a thymidine analog 5-ethynyl-2'-deoxyuridine (EdU) using an EdU cell proliferation kit (Beyotime, Shanghai, China). The cultured fibroblasts were incubated on 6-well plates and labeled with 10 μM EdU for 6 hours after BSA or AGE-BSA treatment. After discarding the culture solution, fibroblasts were incubated in 4% paraformaldehyde for 20 min at ambient temperature. Then fibroblasts were incubated with 0.3% Triton X-100 for 10 min at ambient temperature. Click additive solution was prepared by blending the click reaction buffer, CuSO4, 488 Azide according to the instructions. And then click additive solution was added into cell culture dishes, incubating for 30 min in dark. Then the Hoechst 33342 was added to cell culture dishes, incubating for 30 min in dark. Fluorescent images were captured using a fluorescence microscope (Leica, Wetzlar, Germany). EdU positive cell rate was calculated by Image J software (1.40g, Wayne Rasband National Institutes of Health, USA). The cell proliferation rates were calculated as the ratio of EdU positive nuclei number to total nuclei number.

2.6. Contractility assay

The contractile activity of fibroblasts was determined by cell-mediated collagen gel contraction assay according to the method previously reported (*30*). 1.0 mg/mL type I rat tail collagen solution (BD Biosciences) was prepared by adding 1 M NaOH, to adjust the final pH value to 7.2. The adherent cells were digested and resuspended in PBS to obtain the final cell concentration. The appropriate number of fibroblasts was then transferred to the neutralized collagen solution. Then the mixture was incubated on ice for 5 min and was pipetted into 12-well culture dishes. The gel coagula were then gently detached from the bottom of the well after being incubated for 1 h at 37°C. A DMEM solution with 50 μg/mL BSA, 50 μg/mL AGE-BSA, or 20 μM quercetin (Sigma) was added to each well. Then cells were static cultured and the gels were observed periodically. Maximum effects on gel contraction were obtained within 72 hours of culture. A chemiluminescence imager was used to take pictures and record gel shrinkage at 0, 24, 48, and 72 hours after the culture. The area of each gel was measured using Image J, and the area proportion of each gel compared to its initial area was calculated. The percentage of gel area to the initial gel area was calculated. The area proportion was inversely proportional to the cell-mediated collagen contractile capacity.

2.7. Intracellular ROS quantification

The intracellular ROS levels were determined by measuring the fluorescent dichlorofluorescein (DCF) using a ROS assay kit (Beyotime). Fluorescent DCF was transformed from the cell-permeable 2', 7' dichlorofluorescein diacetate (DCFH-DA) under oxidation by intracellular ROS. Before loading DCFH-DA, cells were treated with 50 μg/mL BSA, 50 μg/mL AGE-BSA, or 20 μM quercetin for 24 hours. Then, the culture medium was replaced by DMEM with 10 μM DCFH-DA, and cells were incubated at 37°C for 30 min. The culture media were removed and cells were washed using DMEM. Then DCF fluorescence distribution was detected by fluorescence microscope or analysis by flow cytometry after cell collection at the wavelength of 488 nm/535 nm.

2.8. Cell transfection

Fibroblasts were cultured in a 6-well plate with complete medium without antibiotics. Once achieving 40-50% confluence, the complete medium was replaced by 1.5 mL/well preheated serum-free DMEM medium. Then, miR-4429 inhibitor or negative control (NC) was diluted by Opti-MEM (Gibco) (15 μL miR-4429 inhibitor or inhibitor NC in 250 μL Opti-MEM) and blended with diluted Lipofectamine 2000 (Thermo Fisher Scientific, Waltham, MA, USA) (5 μL Lipofectamine 2000 in 250 μL Opti-MEM). The mixture was thoroughly mixed and stood for 20 minutes at ambient temperature, and then it was carefully added to the culture medium, 500 μL/well. The 6-well plates were static cultured for 6 hours. Then the culture medium was replaced by the completed culture medium and the cells were continued to culture for 24-48 hours before they were used in the subsequent experiments. The sequences of miR-4429 inhibitor and inhibitor-NC were listed in Table 1.

Table 1. Primer sequences

Name	Sequence (5' to 3')
COL1 forward	GTGCGATGACGTGATCTGTGA
COL1 reverse	CGGTGGTTTCTTGGTCGGT
COL3 forward	GGTAGTCTCACAGCCTTGCG
COL3 reverse	GAGGATGGTTGCACGAAACAC
COL5 forward	TCCGAAGGGGCCAGAATCA
COL5 reverse	GAGCAGTTTCCCACGCTTGA
MMP1 forward	GGGGCTTTGATGTACCCTAGC
MMP1 reverse	TGTCACACGCTTTTGGGGTTT
MMP3 forward	ATGAACAATGGACAAAGGATACAACAG
MMP3 reverse	CATCTTGAGACAGGCGGAACC
TIMP1 forward	CTTCTGCAATTCCGACCTCGT
TIMP1 reverse	ACGCTGGTATAAGGTGGTCTG
Elastin forward	CCTCCCTTCTGCTTCCTCTC
Elastin reverse	CGACTGTTCTTTCGCTGCTG
LOX forward	GGCGAAGGGTGAGGAGTAAG
LOX reverse	TGGGAGACCTAAACGTCAGC
LOXL1 forward	TATGTCCAGAGAGCCCACCT
LOXL1 reverse	TAGCACCCGCACATCGTAGT
LOXL2 forward	ATGTCACCTGCGAGAATGGG
LOXL2 reverse	TGCTCTGGCTTGTACGCTTT
FBN2 forward	CTCTTCTTCTGGGGGCGACTT
FBN2 reverse	CGCTCCGAAGACGGATATTGG
FBLN5 forward	TCTGGAAAGGGCAGCAACTT
FBLN5 reverse	CTTGTCTATCAGCCGATGCG
CASP3 forward	CCAAAGATCATACATGGAAGCG
CASP3 reverse	CTGAATGTTTCCCTGAGGTTTG
PTEN forward	TTTTGAAGACCATAACCCAC
PTEN reverse	TATCATTACACCAGTTCGTC
GAPDH forward	GGAGCGAGATCCCTCCAAAAT
GAPDH reverse	GGCTGTTGTCATACTTCTCATGG
miR-4429 inhibitor	CGCCUCUCAGCCCAGCUUUU
inhibitor NC	UCUACUCUUUCUAGGAGGUUGUGA

COL, collagen; MMP, matrix metalloproteinase; TIMP, tissue inhibitor of matrix metalloproteinase; LOX, lysyl oxidase; LOXL, lysyl oxidase like protein; FBN, fibrilin; FBLN, fibulin; CASP, caspase; PTEN, phosphatase and tensin homolog; GAPDH, glyceraldehyde-3-phosphate dehydrogenase; NC, negative control.

2.9. Western blotting

The cultured fibroblasts were treated by lysis buffer (Beyotime). Total proteins were extracted by centrifugation and were separated under electrophoresis. Separate proteins were transferred to polyvinylidene fluoride membranes. The blocking solution was 5% bovine serum albumin (Sigma) or nonfat-dried milk/TBST. Then, membranes were successively incubated with the primary and secondary antibodies under optimal conditions. The antibodies in the present study included anti-PI3K antibody, anti-pan-Akt antibody, anti-phosphorylated Akt (S473) antibody (Cell Signaling Technology, Danvers, MA, USA), anti-PTEN antibody, and anti-GAPDH antibody (Abcam, Cambridge, MA, USA). After being washed completely, the membrane was covered by an appropriate amount of chemiluminescence reagent (Merck Millipore, Billerica, MA, USA) to carry out the enhanced chemiluminescence. Relative intensities of the images were measured by Image J (1.40 g, USA).

2.10. Quantitative polymerase chain reaction (qPCR)

Total RNA was extracted by an RNA purification kit (EZBioscience, Roseville,CA, USA) from the fibroblasts which were cultured under different indicated treatments. The concentration of RNA was determined by NanoDrop Spectrophotometer (Thermo Fisher Scientific). Then RNA was converted into cDNA by reverse transcription. After the qPCR system was prepared using SYBR Green qPCR master mix (Takara, Tokyo, Japan), the mixture was thoroughly mixed and pipetted into a 384-well plate. The expressions of target genes at the mRNA level were detected by the QuantStudio Flex Real-Time PCR System (Thermo Fisher Scientific). The valid cycle threshold values were collected from each group's data. The expression of GAPDH was considered as the internal reference, and the relative gene expression was calculated by the $2^{(-\Delta\Delta CT)}$ method. All of the primer sequences in the present study were shown in Table 1.

2.11. Statistical analysis

Student's *t*-test was conducted to calculate the statistic difference between two groups when the data obey normal distribution with equal standard deviations. When the data did not obey normal distribution, Mann-Whitney test was applied for the contrast between two groups. The significant differences between 3 or more groups were identified by ANOVA, and Tukey test was applied to determine the significant differences in pairs. Differences were regarded as statistically significant when $p < 0.05$. All the tests were calculated by the GraphPad Prism software (Version 9).

3. Results

3.1. Quercetin inhibited AGEs-induced fibroblast apoptosis

The apoptotic rate in fibroblasts exposed to AGE-BSA was significantly higher than that in fibroblasts exposed to BSA. This AGEs-induced fibroblast apoptosis was inhibited by quercetin with concentrations of 20 μM, 40 μM, 80 μM, and 160 μM for 24 hours (Figures 1A and 1B). Similarly, the gene expression of caspase-3 was upregulated by AGE-BSA, and this upregulation was reversed by quercetin with concentrations of 20 μM, 40 μM, and 80 μM for 24 hours (Figure 1C). To evaluate the inhibitory effects of quercetin with different exposure duration in AGEs-induced fibroblast apoptosis, the fibroblasts treated with AGE-BSA were subsequently treated with 20 μM quercetin for 12, 24, 36, and 48 hours. The AGEs-induced cell apoptosis was inhibited by quercetin in 12, 24, 36, and 48 hours groups (Figures 1D and 1E). Therefore, the optimum condition of quercetin as an antagonist to AGEs in fibroblast apoptosis was 20 μM for 24 hours, which was applied in the following experiments.

3.2. Quercetin antagonized the inhibiting effect of AGEs on cell proliferation

To determine the influence of AGEs on cell proliferation, we assessed the level of EdU in fibroblasts exposed to 50 μg/mL AGE-BSA or BSA (Figure 2A). The proliferation rates were calculated and illustrated (Figure 2B). As shown in Figures 2A and 2B, the proliferation rate was apparently reduced in the AGE-BSA treated groups compared with the BSA treated group both in fibroblasts from POP tissues or fibroblasts from non-POP tissues. And there was no significant difference between the fibroblasts from POP and non-POP groups exposed to BSA only. Notably, the AGEs-inhibited proliferation rate in fibroblasts of the POP group was reversed by quercetin (Figures 2C and 2D).

3.3. Quercetin inhibited AGEs-induced intracellular ROS increase in fibroblasts

To measure the effect of AGEs on the inner cellular ROS of fibroblasts, we detected the DCF positive cells using a flow cytometer and fluorescence microscope. The positive cell rates were increased both in POP and non-POP groups when treated by AGE-BSA compared to cell samples treated by BSA (Figures 3A-3C). And there was no significant difference in positive cell rates between fibroblasts from the POP and non-POP groups. Noticeably, AGEs-induced intracellular ROS increase was inhibited by quercetin, for the positive cell rate inhibition was alleviated by quercetin in fibroblasts from the POP group (Figures 3D-3F).

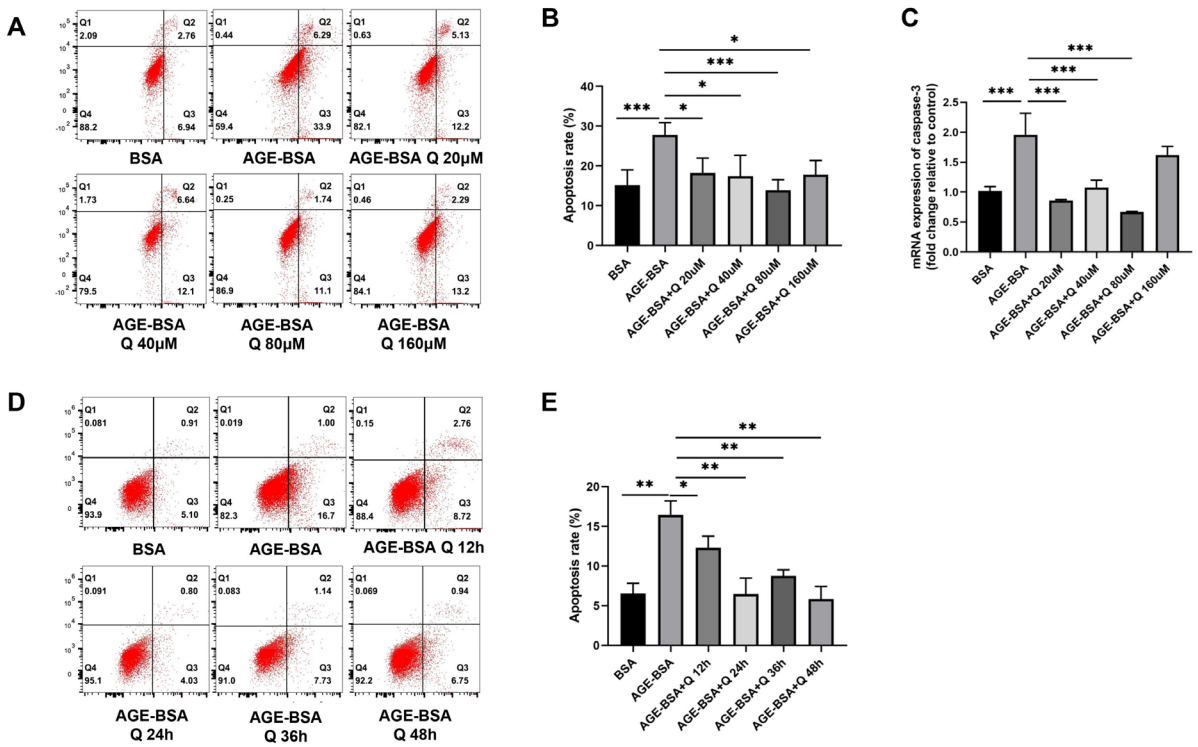

Figure 1. Quercetin inhibited AGEs-induced fibroblast apoptosis. (A) Flow cytometry analysis of cell apoptosis in fibroblasts treated by BSA, BSA-AGE, and quercetin with different concentrations. **(B)** The apoptosis rates of fibroblasts treated by BSA, BSA-AGE, and quercetin with different concentrations. **(C)** The mRNA expression of caspase-3 in fibroblasts treated by BSA, BSA-AGE, and quercetin. **(D)** Flow cytometry analysis of cell apoptosis in fibroblasts treated by BSA, BSA-AGE, and quercetin with different durations. **(E)** The apoptosis rates of fibroblasts treated by BSA, BSA-AGE, and quercetin with different durations. Error bars represent mean± SD of 3 independent experiments, *$p < 0.05$, **$p < 0.01$, ***$p < 0.005$. AGE: advanced glycation end products; BSA: bovine serum albumin; Q: quercetin; SD: standard deviation.

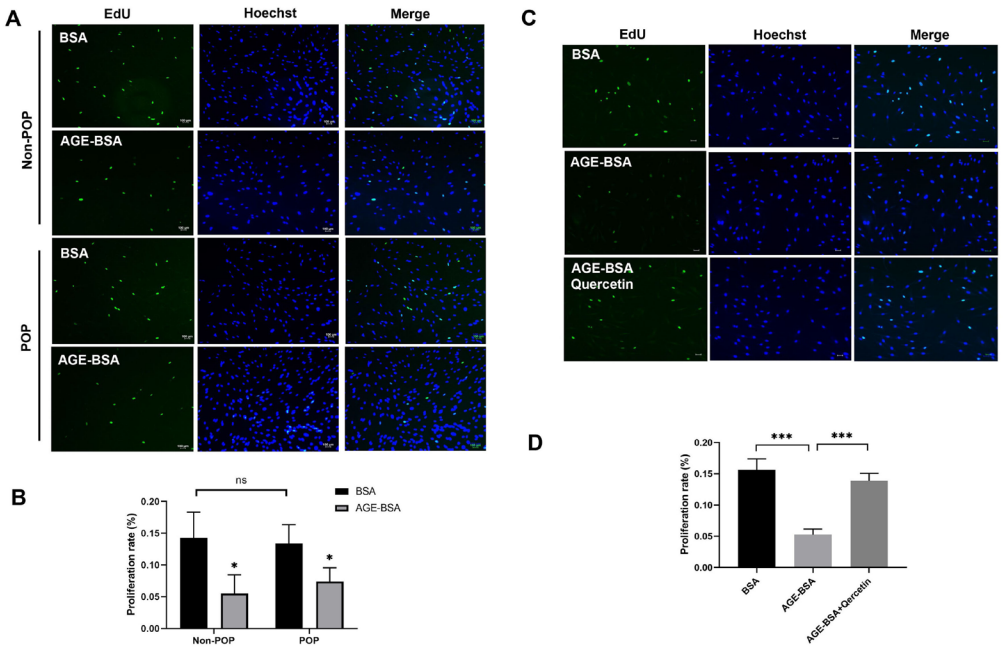

Figure 2. Quercetin alleviated the inhibitory effect of AGEs on cell proliferation. (A) The level of EdU in fibroblasts treated with AGE-BSA or BSA. **(B)** The cell proliferation rates in fibroblasts treated with AGE-BSA or BSA. **(C)** The level of EdU in fibroblasts treated with BSA, AGE-BSA, and quercetin. **(D)** The cell proliferation rates in fibroblasts treated with BSA, AGE-BSA, and quercetin. Error bars represent mean± SD of 3 independent experiments, *$p < 0.05$, ***$p < 0.005$. Scar bar: 100μm. AGE: advanced glycation end products; BSA: bovine serum albumin; POP: pelvic organ prolapse; EdU: 5-ethynyl-2'-deoxyuridine; SD: standard deviation.

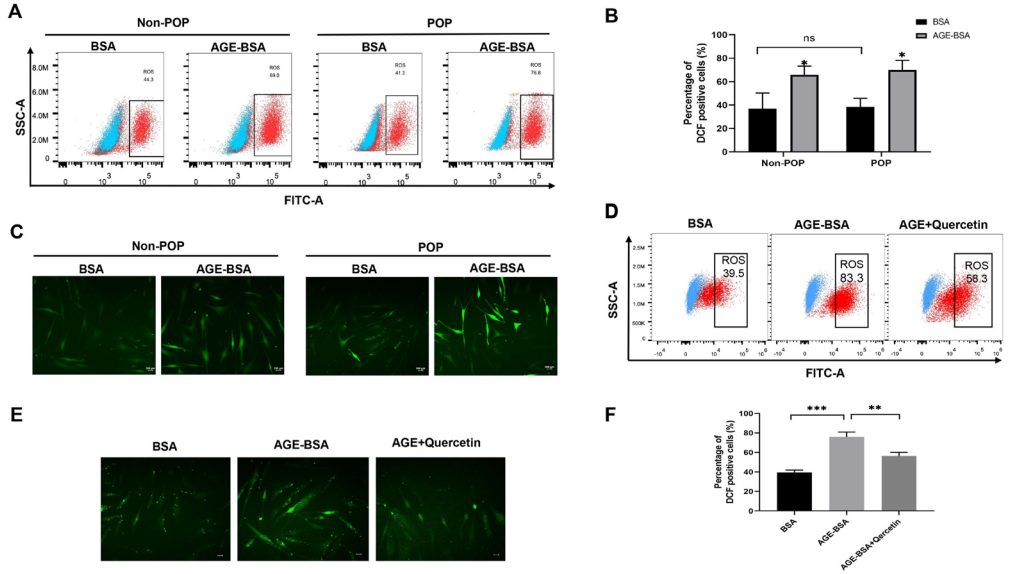

Figure 3. Quercetin inhibited AGEs-induced intracellular ROS increase in fibroblasts. (A) Flow cytometry analysis of DCF-positive cells in fibroblasts treated with AGE-BSA or BSA. **(B)** Percentage of DCF-positive cells in fibroblasts treated with AGE-BSA or BSA. **(C)** The level of DFC in fibroblasts treated with AGE-BSA or BSA. **(D)** Flow cytometry analysis of DCF-positive cells in fibroblasts treated with BSA, AGE-BSA, and quercetin. **(E)** The level of DFC in fibroblasts treated with BSA, AGE-BSA, and quercetin. **(F)** Percentage of DCF-positive cells in fibroblasts treated with BSA, AGE-BSA, and quercetin. Error bars represent mean± SD of 3 independent experiments, *$p < 0.05$, **$p < 0.01$, ***$p < 0.005$. Scar bar: 100μm. AGE: advanced glycation end products; BSA: bovine serum albumin; POP: pelvic organ prolapse; FITC-A: fluorescein isothiocyanate-area; SSC-A: side scatter-area; ROS: reactive oxygen species; DCF: dichlorofluorescein; ns: no significance; SD: standard deviation.

3.4. Quercetin did not improve the contractile impairment of fibroblasts induced by AGEs

We assessed whether AGEs and quercetin affect the contractility of fibroblasts by evaluating the cell-induced gel contraction of type I collagen. Results showed that cell contractility was impaired in fibroblasts from the POP group compared with the non-POP group (Figures 4A and 4B). In addition, treatment with AGE-BSA was found to significantly block the contractile activity of fibroblasts compared to BSA-treated cells in the non-POP group (Figures 4A and 4B). In the POP group,

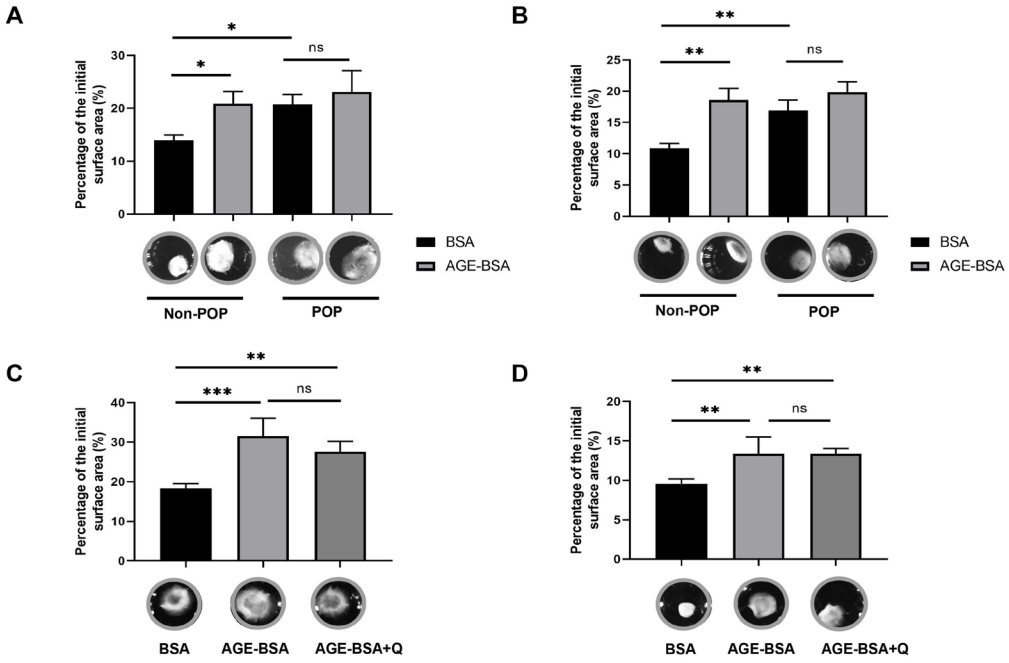

Figure 4. Quercetin did not improve the contractile impairment of fibroblasts induced by AGEs. (A) Percentage of the initial surface area in fibroblasts treated with AGE-BSA or BSA for 48 hours. **(B)** Percentage of the initial surface area in fibroblasts treated with AGE-BSA or BSA for 72 hours. **(C)** Percentage of the initial surface area in fibroblasts treated with BSA, AGE-BSA, and quercetin for 48 hours. **(D)** Percentage of the initial surface area in fibroblasts treated with BSA, AGE-BSA, and quercetin for 72 hours. Error bars represent mean± SD of 3 independent experiments; $*p < 0.05$, $**p < 0.01$, $***p < 0.005$. AGE: advanced glycation end products; BSA: bovine serum albumin; Q: quercetin; POP: pelvic organ prolapse; ns: no significance; SD: standard deviation.

although there was a trend that fibroblasts treated by AGE-BSA exhibited impaired contractility, there was no statistical difference between fibroblasts treated by AGE-BSA and BSA. Therefore, fibroblasts from the POP group were used for assessing the effects of quercetin on cell contractility. Results showed that the AGEs-induced cell contractility impairment was not influenced by quercetin in fibroblasts from the non-POP group (Figures 4C and 4D).

3.5. Quercetin partially reversed AGEs-induced imbalance of ECM gene expression in fibroblasts

To investigate whether quercetin antagonizes AGEs-induced disordered ECM production of fibroblasts, the expression of collagen and elastin-related genes in fibroblasts exposed to quercetin and AGE-BSA or BSA were assessed by qPCR. There was no statistical difference between collagen-related genes in fibroblasts from the POP and non-POP groups (Figures 5A-5F). AGE-BSA downregulated the expressions of COL1 (collagen type 1) both in the POP and non-POP groups (Figure 5A). AGE-BSA downregulated TIMP1 (tissue inhibitor of matrix metalloproteinase 1) expression and upregulated MMP1 expression of fibroblasts in the POP group (Figures 5D and 5F). Quercetin reversed AGEs-induced upregulation of MMP1, but not influenced the expressions of AGEs-downregulated COL1 and TIMP1 in fibroblasts from the POP group (Figures 5G-5I). For elastin-related genes, results showed that the expressions of LOX, LOXL2, FBN2, and FBLN5 decreased, and the expression of LOXL1 increased in fibroblasts from the POP group compared with the non-POP group (Figures 6A-6F). AGE-BSA upregulated the expressions of elastin and FBLN5 in fibroblasts from both the POP and non-POP groups. Quercetin increased the expressions of LOX, and FBN2, and decreased the expression of LOXL1 in fibroblasts from the POP group, suggesting that quercetin reduced the expression differences of LOX, FBN2, and LOXL1 between the POP and non-POP group (Figures 6G-6L). However, the disorders of elastin and FBLN5 expression induced by AGEs were not reversed by quercetin.

3.6. Quercetin inhibited AGEs induced apoptosis of fibroblasts *via* miR-4429 /PTEN/PI3K/Akt

Next, we assessed the influences of quercetin on the expressions of PTEN, PI3K, phosphorylated Akt (p-Akt), and miR-4429 in AGEs-treated fibroblasts. Results showed that AGEs suppressed the expressions of PI3K and p-Akt but increased the expression of PTEN. Quercetin with a concentration of 20 μM effectively antagonized the influences of AGEs on the expressions of PI3K, p-Akt, and PTEN in fibroblasts (Figure 7A). AGEs also significantly downregulated the expression of miR-4429, and the decreased expression of miR-4429 was reversed by 20 μM quercetin (Figure 7B).

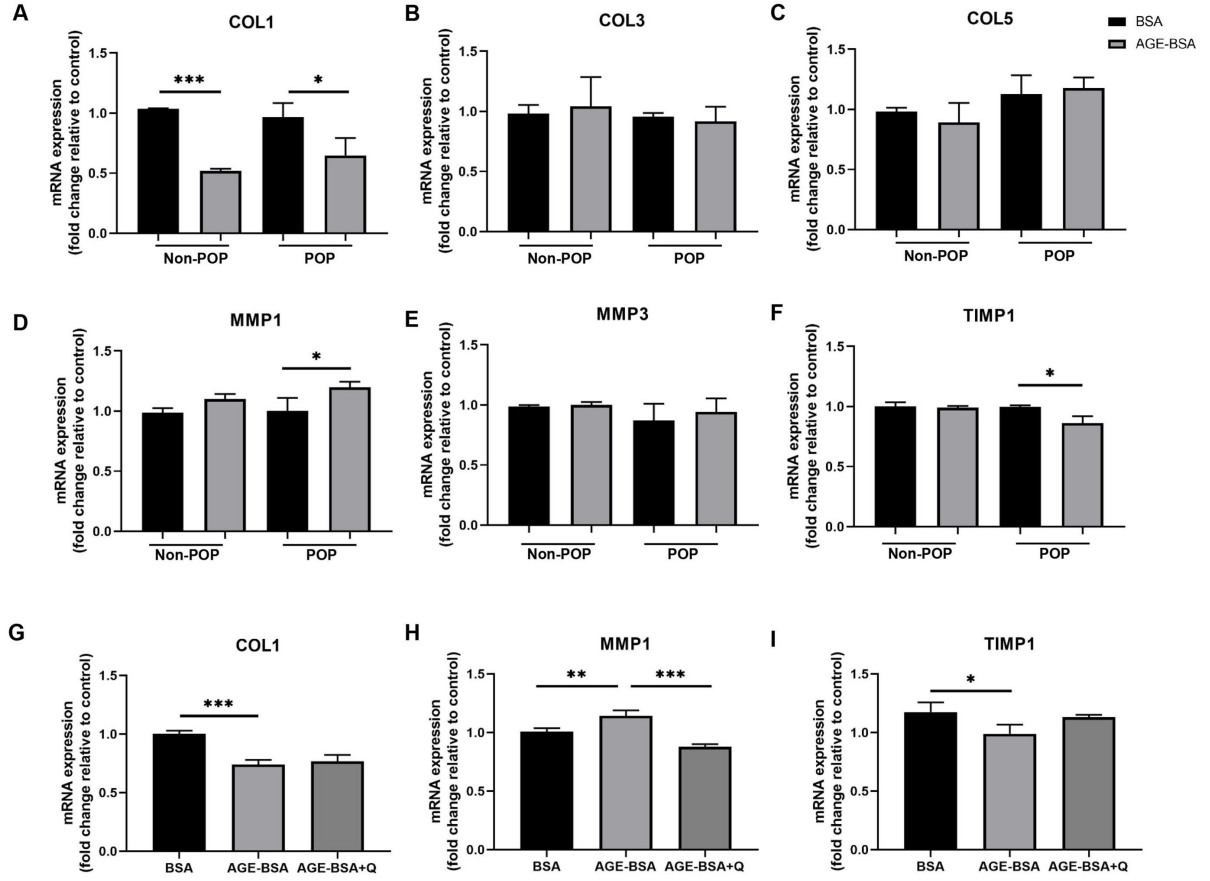

Figure 5. Effects of quercetin on AGEs-induced imbalance of collagen-related gene expression in fibroblasts. (A-F) The mRNA expression of COL1, COL3, COL5, MMP1, MMP3, and TIMP1 in fibroblasts treated with BSA or AGE-BSA. **(G-I)** The mRNA expression of COL1, MMP1, and TIMP1 in fibroblasts treated with BSA, AGE-BSA, and quercetin. Error bars represent mean± SD of 3 independent experiments; *$p<0.05$, **$p<0.01$, ***$p<0.005$. COL: collagen; MMP, matrix metalloproteinase; TIMP, tissue inhibitor of matrix metalloproteinase; AGE: advanced glycation end products; BSA: bovine serum albumin; Q: quercetin; POP: pelvic organ prolapse; SD: standard deviation.

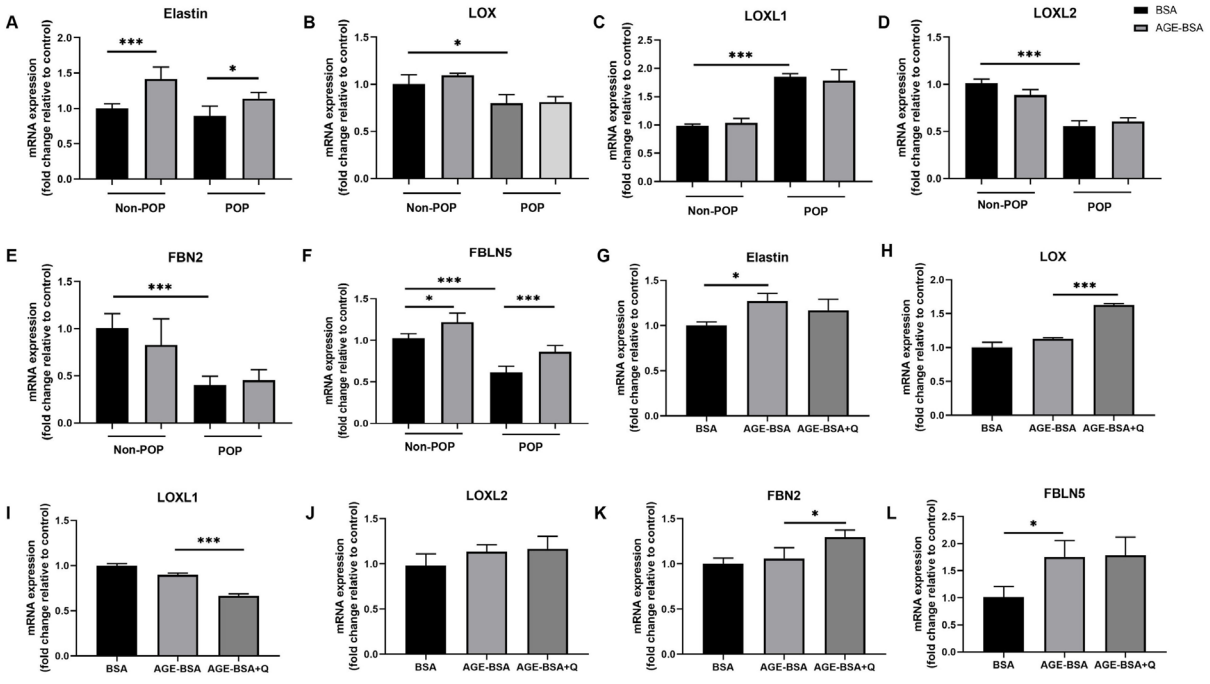

Figure 6. Effects of quercetin on AGEs-induced imbalance of elastin-related gene expression in fibroblasts. (A-F) The mRNA expression of elastin, LOX, LOXL1, LOXL2, FBN2, and FBLN5 in fibroblasts treated with BSA or AGE-BSA. **(G-L)** The mRNA expression of elastin, LOX, LOXL1, LOXL2, FBN2, and FBLN5 in fibroblasts treated with BSA, AGE-BSA, and quercetin. Error bars represent mean± SD of 3 independent experiments; *$p<0.05$, ***$p<0.005$. LOX, lysyl oxidase; LOXL, lysyl oxidase like protein; FBN, fibrilin; FBLN, fibulin; AGE: advanced glycation end products; BSA: bovine serum albumin; Q: quercetin; POP: pelvic organ prolapse; SD: standard deviation.

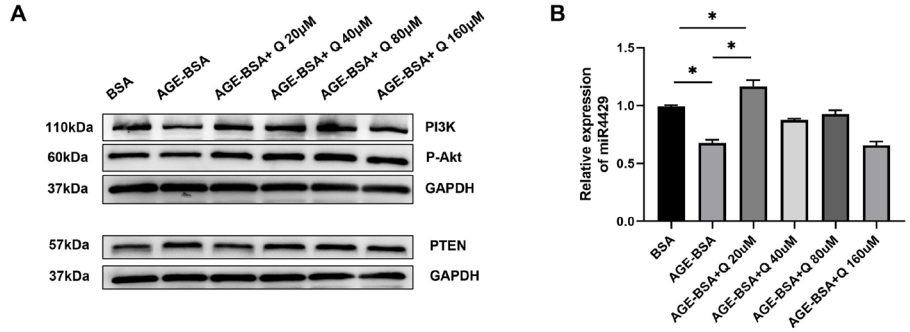

Figure 7. Quercetin antagonized AGEs-induced abnormal expressions of PTEN, PI3K, Akt, and miR-4429 in fibroblasts. (A) Western blot analysis of PI3K, P-Akt, and PTEN in fibroblasts treated with BSA, AGE-BSA, and quercetin with different concentrations. **(B)** The expression of miR-4429 in fibroblasts treated with BSA, AGE-BSA, and quercetin with different concentrations. Error bars represent mean± SD of 3 independent experiments; *$p<0.05$. PI3K: phosphoinositide 3-kinase; P-Akt: phosphorylated Akt; PTEN: phosphatase and tensin homolog; GAPDH: glyceraldehyde-3-phosphate dehydrogenase; BSA: bovine serum albumin; AGE: advanced glycation end products; Q: quercetin; SD: standard deviation.

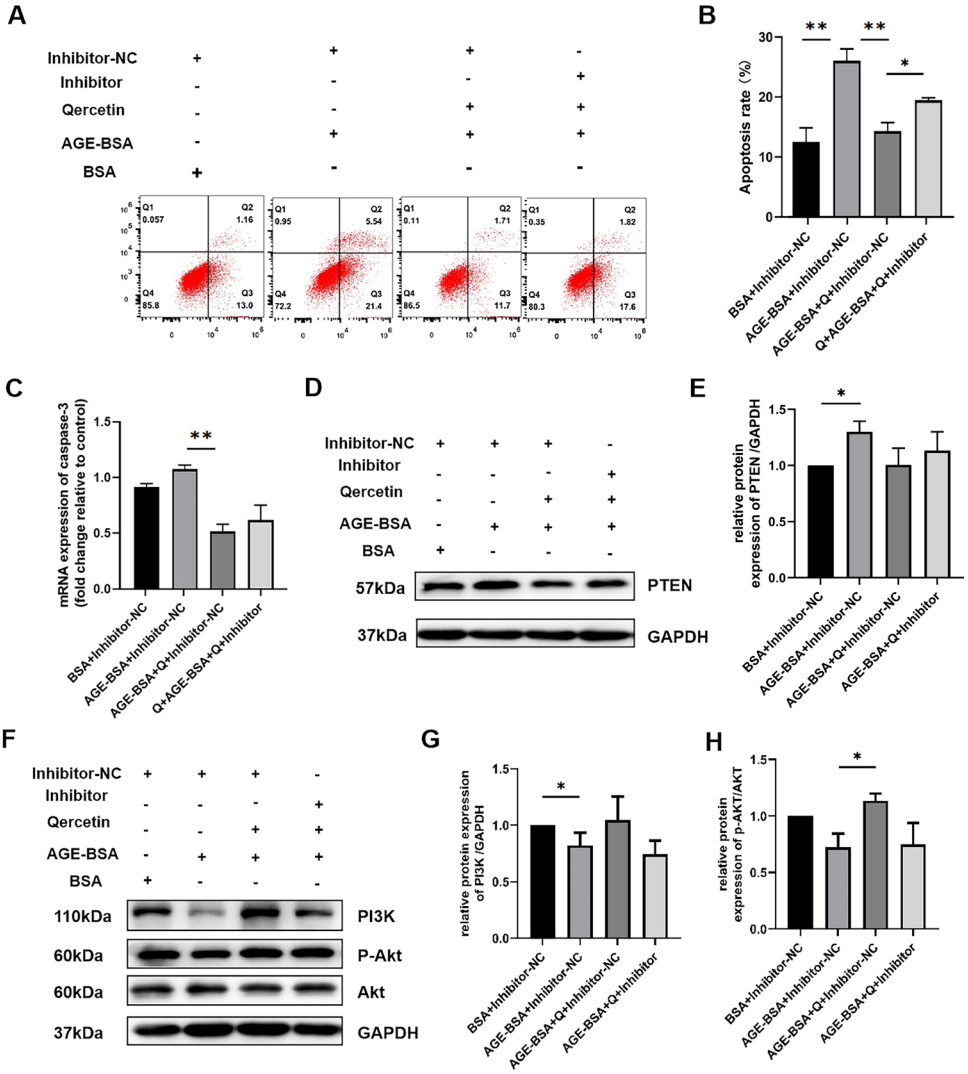

Figure 8. Quercetin inhibited AGEs induced apoptosis of fibroblasts *via* miR-4429 /PTEN/PI3K/Akt. (A) Flow cytometry analysis of cell apoptosis in fibroblasts transfected with miR-4429 inhibitor or inhibitor-NC, treated with BSA, BSA-AGE, or quercetin. **(B)** The apoptosis rates of fibroblasts transfected with miR-4429 inhibitor or inhibitor-NC, treated with BSA, BSA-AGE, or quercetin. **(C)** The mRNA expression of caspase-3 in fibroblasts transfected with miR-4429 inhibitor or inhibitor-NC, treated with BSA, BSA-AGE, or quercetin. **(D)** The protein expression of PTEN in fibroblasts transfected with miR-4429 inhibitor or inhibitor-NC, treated with BSA, BSA-AGE, or quercetin. **(E)** The relative protein expression of PTEN. **(F)** The protein expression of PI3K, Akt, and P-Akt in fibroblasts transfected with miR-4429 inhibitor or inhibitor-NC, treated with BSA, BSA-AGE, or quercetin. **(G)** The relative protein expression of PI3K. **(H)** The relative protein expression ratio of P-Akt/Akt. Error bars represent mean± SD of 3 independent experiments, *$p < 0.05$, **$p < 0.01$. AGE: advanced glycation end products; BSA: bovine serum albumin; Q: quercetin; PTEN: phosphatase and tensin homolog; PI3K: phosphoinositide 3-kinase; Akt: protein kinase B; P-Akt: phosphorylated Akt; GAPDH: glyceraldehyde-3-phosphate dehydrogenase; NC: negative control; SD: standard deviation.

Furthermore, transfection with miR-4429 inhibitor downregulated the expression of miR-4429 in fibroblasts from the POP group, and then the effects of different cell treatment conditions on fibroblast apoptosis were detected. As shown in Figures 8A and 8B, AGE-BSA significantly increased the cell apoptosis rate. Quercetin effectively reversed the increase of cell apoptosis rate and caspase-3 expression induced by AGE-BSA (Figures 8A-8C). However, this antagonistic effect on AGEs of quercetin was weakened by inhibiting the expression of miR-4429 (Figures 8A and 8B). In addition, AGE-BSA upregulated the protein expression of PTEN, which were reversed by quercetin (Figures 8D and 8E). While downregulating the expression of miR-4429, quercetin did not inhibit the protein expression of PTEN. Similarly, quercetin elevated the protein expressions of PI3K and p-Akt that were downregulated under the exposure to AGEs in fibroblasts. And the antagonistic effect of quercetin was diminished by reducing the expression of miR-4429 (Figures 8F-8H).

4. Discussion

The effect of AGEs on fibroblasts has been reported mainly in diabetes mellitus and its complications. AGEs inhibited the proliferation of tendon fibroblasts, leading to tendon pain and degenerative changes (*31*). AGEs induced inflammation and overexpression of fibrotic genes, resulting in diabetic fibrosis (*32*). AGEs accumulation in skin resulted in collagen structural damages and fibroblast apoptosis, collagen degradation in diabetes non-healing wounds (*33*). However, the effects of AGEs on the behavior and function of pelvic floor fibroblasts are rarely studied. This study comprehensively explored the effects of AGEs on the behavior and function of pelvic floor fibroblasts and found that quercetin could antagonize the inhibitory effects of AGEs on the behavior and function of pelvic floor fibroblasts in terms of cell proliferation, apoptosis, oxidative stress, and ECM metabolism.

Firstly, the proliferation rates of fibroblasts were detected and there was no significant difference in proliferation ability between the POP and non-POP groups, which was consistent with a previous report (*34*). We found that quercetin antagonized the decrease in the proliferation rate of fibroblasts induced by AGEs. Studies on the influences of quercetin on fibroblasts suggest that quercetin may be applied in the treatment of rheumatoid arthritis and fibrotic diseases due to its anti-inflammatory and anti-fibrotic effects (*22,35*). In addition, quercetin delayed the senescence of human dermal fibroblasts induced by UV irradiation (*36*). However, the effect of quercetin on pelvic floor fibroblasts is rarely studied. And in the present study, we hypothesized that quercetin could antagonize AGEs-induced apoptosis and functional inhibition of fibroblasts from the prolapsed uterosacral ligament.

In this study, we found that AGEs increased the ROS levels in fibroblasts, while quercetin effectively alleviated this oxidative stress status. Oxidative stress was reported as a negative factor in the pathogenesis of POP, and the previous results showed that oxidative stress status existed in prolapsed tissues (*37,38*). Increased production and decreased elimination of intracellular ROS leads to oxidative stress, an imbalance between intracellular oxidants and antioxidants (*39*). The antioxidant effect of quercetin has been widely reported and quercetin prevented myocardial fibrosis and diabetic nephropathy by inhibiting ROS production (*18,40*).

The contractility of fibroblasts is crucial for regulating connective tissue remodeling during normal and pathological wound healing (*41*). Meyer *et al*. preliminarily demonstrated that myofibroblasts of vaginal wall tissue derived from POP had impaired contractile ability by cell-mediated collagen gel contractility assay, and their contractile ability decreased with age (*42*). Ruiz-Zapata *et al.* reported that the fibroblasts derived from the POP tissues exhibited delayed contractility compared with the normal fibroblasts (*6*). In our study, the contractility of fibroblasts from the POP group was inferior to that in the non-POP group, and AGEs treatment significantly damaged cell contractility in fibroblasts of the non-POP group. However, quercetin did not antagonize AGEs-induced contractility decrease in fibroblasts, suggesting quercetin did not influence the contractile-related molecules in fibroblasts.

Dysfunctions of fibroblasts lead to dysregulated metabolism of collagen, elastin, and other ECM-related genes, resulting in the damaged mechanical strength of pelvic connective tissues and contributing to the development of POP (*43*). The extracellular matrix proteins have been detected in human tissues such as the vaginal wall and the uterosacral ligament, and there were significant differences between the prolapsed and normal tissues, indicating that ECM alterations are correlated with POP (*44,45*). Considering that the formation and remodeling of ECM are regulated by fibroblasts, the related gene expressions of fibroblasts were quantified in this study.

The ECM of pelvic connective tissue is mainly consisted of the most abundant type I and III collagen that provide the primary tensile resistance to connective tissue. In the pathological alterations of POP, collagen was reported with a decreased content in POP. MMP1, as a kind of degrading enzyme of collagen was increased in POP, and reversely, TIMP1 as the inhibitor of MMP was decreased in POP (*46*). In this study, the collagen expression of the POP group was not significantly different from the non-POP group, which was different from the previous reports. The reason for the result may be that the fibroblasts were detached from the *in-vivo* environment with high AGEs concentration or the sample size in the experiment was too small. AGEs downregulated the expression of COL1 and TIMP1

but increased the expression of MMP1 in the POP group. This result coincides with our previous report (*16*), suggesting that AGEs decreased the expression of COL1 by increasing the degradation of COL1. The previous studies revealed that quercetin downregulated the expression of MMP2 and MMP9 to prevent fibrosis and contributed to wound healing (*47,48*). Our results suggested that quercetin antagonized AGEs-induced upregulation of MMP1 in fibroblasts.

Elastin is another important fibrous structural protein and constitutes the elastic fiber of ECM, allowing the pelvic floor connective tissue with high extensibility and passive retraction. The molecules including LOX, LOXL, FBLN, and FBNs are correlated with the composition of elastic fibers and the synthesis of elastin (*49*). Animal studies demonstrated that the knockout of *LOXL1*, *FBLN3*, and *FBLN5* resulted in rectal or vaginal prolapse in mice (*50*). However, few studies have focused on the influence of AGEs or quercetin on elastin metabolism in pelvic floor fibroblasts. Our results showed that the gene expressions of LOX, LOXL2, FBN2, and FBLN5 were reduced in fibroblasts from the POP group compared with the non-POP group, which was in line with the previous reports that the *FBLN5* knockout mice exhibited organ prolapse (*50*). AGEs treatment promoted the expressions of Elastin and FBLN5 in fibroblasts, while AGEs did not influence the expression of LOX, LOXL1, LOXL2, and FBN2. Quercetin promoted the expressions of LOX and FBN2, while inhibiting the expression of LOXL1, which means quercetin reduced the expression differences of *LOX*, *FBN2*, and *LOXL1* genes between the POP group and non-POP group. But quercetin had no significant effect on the expressions of Elastin and FBLN5 in POP fibroblasts induced by AGEs.

Confirming the antagonistic effects of quercetin on AGEs, we tried to understand the molecular process of the antagonism of quercetin on AGEs-induced fibroblast apoptosis. Our previous study indicated that AGEs induced fibroblast apoptosis by increasing the expression of PTEN (*17*). The expression of PTEN was post-transcriptionally regulated by miR-4429, and then the upregulation of PTEN did antagonize the PI3K/Akt pathway, which consequently increased cell apoptosis. In the current study, quercetin significantly antagonized the influences of AGEs on fibroblasts, including the upregulation of cell apoptosis and PTEN expression, and the downregulation of miR-4429, PI3K, and phosphorylated Akt expression. Furthermore, the antagonistic effects of quercetin on AGEs were neutralized by inhibiting the expression of miR-4429.

The limitation of our study is the lack of *in vivo* experiments to verify the effects and mechanism of quercetin in the treatment of POP. Humans are strictly biped, and the direction in which the pelvic organs are subjected to gravity differs from that of model animals commonly used in laboratories. Besides, vaginal delivery in humans causes more serious damage to pelvic floor structures than in other species. Therefore, we plan to test and select the most appropriate animal model to explore whether quercetin improves the functional damage of AGEs to fibroblasts *in vivo*, and further verify the molecular mechanism at the cellular level found in the present study.

In summary, quercetin antagonized AGE-induced apoptosis, proliferation inhibition, and ROS increase in fibroblasts, but not AGEs-induced contractile impairment in fibroblasts. Quercetin partially improved the expression disorder of ECM-related genes in fibroblasts induced by AGEs. Furthermore, quercetin reduced fibroblasts apoptosis in POP through reversing AGEs-induced downregulation of miR-4429, upregulation of PTEN, and downregulation of PI3K/Akt.

Acknowledgements

We gratefully acknowledge the assistance of Jing Zhou in preparing the manuscript.

Funding: This study was supported by Science and Technology Commission of Shanghai Municipality (grant no. 20Y11907300 and 21Y11906700 to YS Chen), the Scientific and Technological Innovation Action Plan of the Shanghai Natural Science Fund (grant no. 20ZR1409100 to L Wang), a project of the Chinese Association of Integration of Traditional and Western Medicine special foundation for Obstetrics and Gynecology-PuZheng Pharmaceutical Foundation (grant no. FCK-PZ-08 to L Wang), a project for hospital management of the Shanghai Hospital Association (grant no. X2021046 to L Wang), and a clinical trial project of the Special Foundation for Healthcare Research of the Shanghai Municipal Health Commission (grant no. 202150042 to L Wang).

Conflict of Interest: The authors have no conflicts of interest to disclose.

References

1. Pang H, Zhang L, Han S, Li Z, Gong J, Liu Q, Liu X, Wang J, Xia Z, Lang J, Xu T, Zhu L. A nationwide population-based survey on the prevalence and risk factors of symptomatic pelvic organ prolapse in adult women in China - a pelvic organ prolapse quantification system-based study. BJOG. 2021; 128:1313-1323.
2. Jelovsek JE, Maher C, Barber MD. Pelvic organ prolapse. Lancet. 2007; 369:1027-1038.
3. Lu Y, Chen HY, Wang XQ, Wang JX. Correlations between Mitofusin 2 expression in fibroblasts and pelvic organ prolapse: an *in vitro* study. Chin Med J (Engl). 2017; 130:2951-2959.
4. Li Y, Hong L, Liu C, Min J, Hong S, Hu M, Zhao Y, Yang Q, Tang J, He S. Effect of puerarin on collagen metabolism of fibroblasts in pelvic tissue of women with pelvic organ prolapse. Mol Med Rep. 2018; 17:2705-2711.
5. Kufaishi H, Alarab M, Drutz H, Lye S, Shynlova O.

Comparative characterization of vaginal cells derived from premenopausal women with and without severe pelvic organ prolapse. Reprod Sci. 2016; 23:931-943.
6. Ruiz-Zapata AM, Kerkhof MH, Zandieh-Doulabi B, Brölmann HA, Smit TH, Helder MN. Functional characteristics of vaginal fibroblastic cells from premenopausal women with pelvic organ prolapse. Mol Hum Reprod. 2014; 20:1135-1143.
7. Feng J, Li Y, Jin X, Gong R, Xia Z. ATF3 regulates oxidative stress and extracellular matrix degradation *via* p38/Nrf2 signaling pathway in pelvic organ prolapse. Tissue Cell. 2021; 73:101660.
8. Jing C, Zhang G, Liu Z, Xu Q, Li C, Cheng G, Shi R. Peroxidasin promotes diabetic vascular endothelial dysfunction induced by advanced glycation end products *via* NOX2/HOCl/Akt/eNOS pathway. Redox Biol. 2021; 45:102031.
9. Zhou Q, Cheng KW, Gong J, Li ETS, Wang M. Apigenin and its methylglyoxal-adduct inhibit advanced glycation end products-induced oxidative stress and inflammation in endothelial cells. Biochem Pharmacol. 2019; 166:231-241.
10. Gkogkolou P, Böhm M. Advanced glycation end products: Key players in skin aging? Dermatoendocrinol. 2012; 4:259-270.
11. Willett TL, Pasquale J, Grynpas MD. Collagen modifications in postmenopausal osteoporosis: advanced glycation endproducts may affect bone volume, structure and quality. Curr Osteoporos Rep. 2014; 12:329-337.
12. Jackson SR, Avery NC, Tarlton JF, Eckford SD, Abrams P, Bailey AJ. Changes in metabolism of collagen in genitourinary prolapse. Lancet. 1996; 347:1658-1661.
13. Chen Y, Huang J, Hu C, Hua K. Relationship of advanced glycation end products and their receptor to pelvic organ prolapse. Int J Clin Exp Pathol. 2015; 8:2288-2299.
14. Sferra R, Pompili S, D'Alfonso A, Sabetta G, Gaudio E, Carta G, Festuccia C, Colapietro A, Vetuschi A. Neurovascular alterations of muscularis propria in the human anterior vaginal wall in pelvic organ prolapse. J Anat. 2019; 235:281-288.
15. Vetuschi A, Pompili S, Gallone A, D'Alfonso A, Carbone MG, Carta G, Festuccia C, Gaudio E, Colapietro A, Sferra R. Immunolocalization of advanced glycation end products, mitogen activated protein kinases, and transforming growth factor-β/smads in pelvic organ prolapse. J Histochem Cytochem. 2018; 66:673-686.
16. Chen YS, Wang XJ, Feng W, Hua KQ. Advanced glycation end products decrease collagen I levels in fibroblasts from the vaginal wall of patients with POP *via* the RAGE, MAPK and NF-κB pathways. Int J Mol Med. 2017; 40:987-998.
17. Sima Y, Li L, Xiao C, Xu L, Wang L, Chen Y. Advanced glycation end products (AGEs) downregulate the miR-4429/PTEN axis to promote apoptosis of fibroblasts in pelvic organ prolapse. Ann Transl Med. 2022; 10:821.
18. Ding T, Wang S, Zhang X, Zai W, Fan J, Chen W, Bian Q, Luan J, Shen Y, Zhang Y, Ju D, Mei X. Kidney protection effects of dihydroquercetin on diabetic nephropathy through suppressing ROS and NLRP3 inflammasome. Phytomedicine. 2018; 41:45-53.
19. Ferenczyova K, Kalocayova B, Bartekova M. Potential implications of quercetin and its derivatives in cardioprotection. Int J Mol Sci. 2020; 21:1585.
20. Smith MJ, Fowler M, Naftalin RJ, Siow RCM. UVA irradiation increases ferrous iron release from human skin fibroblast and endothelial cell ferritin: Consequences for cell senescence and aging. Free Radic Biol Med. 2020; 155:49-57.
21. Li C, Shen Y, Huang L, Liu C, Wang J. Senolytic therapy ameliorates renal fibrosis postacute kidney injury by alleviating renal senescence. FASEB J. 2021; 35:e21229.
22. Hohmann MS, Habiel DM, Coelho AL, Verri WA, Jr., Hogaboam CM. Quercetin enhances ligand-induced apoptosis in senescent idiopathic pulmonary fibrosis fibroblasts and reduces lung fibrosis *in vivo*. Am J Respir Cell Mol Biol. 2019; 60:28-40.
23. Huang L, Zhao Z, Wen J, Ling W, Miao Y, Wu J. Cellular senescence: A pathogenic mechanism of pelvic organ prolapse (Review). Mol Med Rep. 2020; 22:2155-2162.
24. Marcu RD, Mischianu DLD, Iorga L, Diaconu CC, Surcel M, Munteanu AN, Constantin C, Isvoranu G, Bratu OG. Oxidative stress: A possible trigger for pelvic organ prolapse. J Immunol Res. 2020; 2020:3791934.
25. Bhuiyan MN, Mitsuhashi S, Sigetomi K, Ubukata M. Quercetin inhibits advanced glycation end product formation *via* chelating metal ions, trapping methylglyoxal, and trapping reactive oxygen species. Biosci Biotechnol Biochem. 2017; 81:882-890.
26. Shimoda H, Nakamura S, Morioka M, Tanaka J, Matsuda H, Yoshikawa M. Effect of cinnamoyl and flavonol glucosides derived from cherry blossom flowers on the production of advanced glycation end products (AGEs) and AGE-induced fibroblast apoptosis. Phytother Res. 2011; 25:1328-1335.
27. Yang S, Wang G, Ma ZF, Qin LQ, Zhai YJ, Yu ZL, Xue M, Zhang YH, Wan Z. Dietary advanced glycation end products-induced cognitive impairment in aged ICR mice: protective role of quercetin. Mol Nutr Food Res. 2020; 64:e1901019.
28. Madhu C, Swift S, Moloney-Geany S, Drake MJ. How to use the pelvic organ prolapse quantification (POP-Q) system? Neurourol Urodyn. 2018; 37:S39-s43.
29. Bump RC, Mattiasson A, Bø K, Brubaker LP, DeLancey JO, Klarskov P, Shull BL, Smith AR. The standardization of terminology of female pelvic organ prolapse and pelvic floor dysfunction. Am J Obstet Gynecol. 1996; 175:10-17.
30. Renthal NE, Chen CC, Williams KC, Gerard RD, Prange-Kiel J, Mendelson CR. miR-200 family and targets, ZEB1 and ZEB2, modulate uterine quiescence and contractility during pregnancy and labor. Proc Natl Acad Sci U S A. 2010; 107:20828-20833.
31. Patel SH, Yue F, Saw SK, Foguth R, Cannon JR, Shannahan JH, Kuang S, Sabbaghi A, Carroll CC. Advanced glycation end-products suppress mitochondrial function and proliferative capacity of achilles tendon-derived fibroblasts. Sci Rep. 2019; 9:12614.
32. Tuleta I, Frangogiannis NG. Diabetic fibrosis. Biochim Biophys Acta Mol Basis Dis. 2021; 1867:166044.
33. Qing C. The molecular biology in wound healing & non-healing wound. Chin J Traumatol. 2017; 20:189-193.
34. Sun B, Zhou L, Wen Y, Wang C, Baer TM, Pera RR, Chen B. Proliferative behavior of vaginal fibroblasts from women with pelvic organ prolapse. Eur J Obstet Gynecol Reprod Biol. 2014; 183:1-4.
35. Sun HT, Li JP, Qian WQ, Yin MF, Yin H, Huang GC. Quercetin suppresses inflammatory cytokine production in rheumatoid arthritis fibroblast-like synoviocytes. Exp Ther Med. 2021; 22:1260.
36. Zou Z, Long X, Zhao Q, *et al*. A single-cell transcriptomic

atlas of human skin aging. Dev Cell. 2021; 56:383-397. e388.
37. Kim EJ, Chung N, Park SH, Lee KH, Kim SW, Kim JY, Bai SW, Jeon MJ. Involvement of oxidative stress and mitochondrial apoptosis in the pathogenesis of pelvic organ prolapse. J Urol. 2013; 189:588-594.
38. Liu C, Yang Q, Fang G, Li BS, Wu DB, Guo WJ, Hong SS, Hong L. Collagen metabolic disorder induced by oxidative stress in human uterosacral ligament-derived fibroblasts: A possible pathophysiological mechanism in pelvic organ prolapse. Mol Med Rep. 2016; 13:2999-3008.
39. Valko M, Leibfritz D, Moncol J, Cronin MT, Mazur M, Telser J. Free radicals and antioxidants in normal physiological functions and human disease. Int J Biochem Cell Biol. 2007; 39:44-84.
40. Min Z, Yangchun L, Yuquan W, Changying Z. Quercetin inhibition of myocardial fibrosis through regulating MAPK signaling pathway *via* ROS. Pak J Pharm Sci. 2019; 32:1355-1359.
41. Tomasek JJ, Gabbiani G, Hinz B, Chaponnier C, Brown RA. Myofibroblasts and mechano-regulation of connective tissue remodelling. Nat Rev Mol Cell Biol. 2002; 3:349-363.
42. Meyer S, Achtari C, Hohlfeld P, Juillerat-Jeanneret L. The contractile properties of vaginal myofibroblasts: is the myofibroblasts contraction force test a valuable indication of future prolapse development? Int Urogynecol J Pelvic Floor Dysfunct. 2008; 19:1399-1403.
43. Zhu Y, Li L, Xie T, Guo T, Zhu L, Sun Z. Mechanical stress influences the morphology and function of human uterosacral ligament fibroblasts and activates the p38 MAPK pathway. Int Urogynecol J. 2022; 33:2203-2212.
44. Zhu YP, Xie T, Guo T, Sun ZJ, Zhu L, Lang JH. Evaluation of extracellular matrix protein expression and apoptosis in the uterosacral ligaments of patients with or without pelvic organ prolapse. Int Urogynecol J. 2021; 32:2273-2281.
45. Eser A, Unlubilgin E, Hizli F, Acar M, Kamalak Z, Kosus A, Kosus N, Hizli D, Gunduz E. Is there a relationship between pelvic organ prolapse and tissue fibrillin-1 levels? Int Neurourol J. 2015; 19:164-170.
46. Hu Y, Wu R, Li H, Gu Y, Wei W. Expression and significance of metalloproteinase and collagen in vaginal wall tissues of patients with pelvic organ prolapse. Ann Clin Lab Sci. 2017; 47:698-705.
47. Yoon JS, Chae MK, Jang SY, Lee SY, Lee EJ. Antifibrotic effects of quercetin in primary orbital fibroblasts and orbital fat tissue cultures of Graves' orbitopathy. Invest Ophthalmol Vis Sci. 2012; 53:5921-5929.
48. Kant V, Jangir BL, Sharma M, Kumar V, Joshi VG. Topical application of quercetin improves wound repair and regeneration in diabetic rats. Immunopharmacol Immunotoxicol. 2021; 43:536-553.
49. Theocharis AD, Skandalis SS, Gialeli C, Karamanos NK. Extracellular matrix structure. Adv Drug Deliv Rev. 2016; 97:4-27.
50. Allen-Brady K, Bortolini MAT, Damaser MS. Mouse knockout models for pelvic organ prolapse: a systematic review. Int Urogynecol J. 2022; 33:1765-1788.

Received July 11, 2023; Revised November 15, 2023; Accepted November 26, 2023.

[§]These authors contributed equally to this work.

*Address correspondence to:
Yisong Chen, Department of Gynecology, Obstetrics and Gynecology Hospital of Fudan University, 419 Fangxie Road, Shanghai, China.
E-mail: cys373900207@163.com

Ling Wang, Laboratory for Reproductive Immunology, Obstetrics and Gynecology Hospital of Fudan University, 419 Fangxie Road, Shanghai, China.
E-mail: Dr.wangling@fudan.edu.cn

Released online in J-STAGE as advance publication December 3, 2023.